Dynamics of the Unload Process for Negative Pressure Sliders

Q. H. Zeng[1], M. Chapin and D. B. Bogy

Computer Mechanics Laboratory
Department of Mechanical Engineering
University of California
Berkeley, CA 94720

ABSTRACT

Dynamic load/unload (L/UL) has been widely used in portable drives and shows great potential in future high performance drives. Negative pressure sliders also have many merit features, but they can develop an undesirable suction force during dynamic unload. In this work the dynamics of negative pressure sliders during the unload process was investigated by simulation and experiment. A simplified L/UL model for the suspension system was created and implemented in the CML dynamic simulator. An experimental setup was built to directly measure the air bearing pull-off forces during unload. Two slider designs have been simulated and measured at various disk rotation speeds. Good correlation between the experimental and simulation results was achieved. During unload the air bearing suction force causes dimple separation. Quick release of the air bearing then results in high speed impact between the slider and load beam, from which, the slider could rebound and hit the disk. By selecting the best rotation speed for unload, we can decrease the amount of dimple separation for a given slider design. The results show that the program and experiment are robust for evaluating the slider air bearing design and unload process. They also point the way to design air bearing surfaces to minimize the pull-off force.

[1] Visiting researcher, Associate professor, Institute of Vibration Engineering, Nanjing University of Aeronautics & Astronautics, Nanjing, China.

I. INTRODUCTION

Dynamic load/unload (L/UL) has been widely used in portable drives, and it shows great potential for future high performance drives. L/UL has many advantages over conventional contact-start-stop (CSS). For example, drives with L/UL mechanisms have better shock resistance, which permits higher non-operating shock. Lower power consumption is achieved by the elimination of stiction forces, which occur during a CSS cycle. Most importantly, no slider-disk wear occurs when L/UL is used if the system is designed to avoid contacts. This enables the use of ultra-smooth disks without a special landing zone and with better overall durability. In addition, the landing zone can be freed up for storing more data. As glide height decreases, the implementation of a landing zone, using laser bumps for example, will be more difficult. Therefore, the disk drive industry is showing an increased interest in L/UL.

Head-disk interface reliability is an important concern of the L/UL system. Jeong and Bogy [1, 2] studied a perpendicular L/UL system by experiment and simulation to find the conditions for avoiding slider-disk impacts. Levi and Talke [3], and Fu and Bogy [4, 5] investigated experimentally the ramp L/UL system. Their research mainly focused on the loading process of positive pressure sliders. The unloading process causes no significant problems for positive pressure sliders, and therefore it was not considered important. However, negative pressure sliders [6] are widely utilized in current drives for many reasons. Such features include faster take-off, less speed sensitivity, better altitude insensitivity, smaller normal load (lower friction and wear during CSS) and lower flying height sensitivity to manufacturing tolerance. However, if negative pressure sliders are used in the L/UL system, the suction force may result in slider-disk contacts during the unload process. More research is required to better understand this phenomenon.

In this paper, we investigated the dynamics of negative pressure sliders during the unload process by simulation and experiment. The CML dynamic simulator [7] was modified to incorporate a simplified L/UL model for the suspension system. In order to directly

measure the air bearing forces during the unload process, we constructed an experimental setup. Two different slider designs were simulated and measured at various RPM's. The experimental results showed good agreement with the simulation results. The air bearing suction forces result in dimple separation. Because of the quick release of the air bearing a high speed impact between the slider and the load beam often occurs. It is possible for the slider to rebound from the load beam and hit the disk. Selecting a suitable RPM can decrease the dimple separation. The results also show that the program and experimental setup are robust for evaluating the slider air bearing design and unload process. It is possible to design sliders to minimize the pull-off force.

II. NUMERICAL MODEL

The experimental results in [5] showed that radial acceleration does not significantly affect slider dynamics during ramp loading, so we ignored the effects of radial motion on the dynamics during the L/UL process. In an actual L/UL system, the suspension is actuated and excited by the airflow in the drive. The suspension dynamics can greatly affect the L/UL process, but it is very difficult to directly include all of the suspension effects in the simulation. The negative pressure sliders can generate very stiff air bearings with resonance frequencies in the range from 40 kHz to 120 kHz for most 50% negative pressure sliders [8, 9]. The suspension assemblies have much lower frequencies. Therefore, during times when the air bearing exists, the effects of the suspension on the slider can be simplified to its static load effects, i.e., the inertial effects of the suspension can be ignored. Thus, the suspension can be modeled as a spring/damper system as shown in Figure 1. During the load process, the effects of suspension vibration can be included in the initial load conditions, such as the initial pitch and roll of the sliders.

Figure 1 shows the model for the L/UL simulation. The governing equations of motion for the slider can be written as

$$m\frac{\mathrm{d}^2 z}{\mathrm{d}t^2} = -f_z + \iint_A (p - p_a)\mathrm{d}A \tag{1}$$

$$I_\theta \frac{\mathrm{d}^2\theta}{\mathrm{d}t^2} + c_\theta \frac{\mathrm{d}\theta}{\mathrm{d}t} + k_\theta \theta = -f_\theta + \iint_A (p - p_a)x\mathrm{d}A \tag{2}$$

$$I_\beta \frac{\mathrm{d}^2\beta}{\mathrm{d}t^2} + c_\beta \frac{\mathrm{d}\beta}{\mathrm{d}t} + k_\beta \beta = -f_\beta + \iint_A (p - p_a)y\mathrm{d}A \tag{3}$$

In Eqs. (1)-(3), z, θ and β are the vertical displacement at the slider's center, and the slider's pitch and roll; m, I_θ and I_β are the mass and moments of inertia of the slider; k_θ, k_β, c_θ, and c_β are stiffness and damping coefficients of the suspension in the pitch and roll directions. f_z is suspension force in the Z-direction, f_θ and f_β are additional suspension forces, p_a is ambient pressure, and p is the pressure governed by the generalized Reynolds equation:

$$\frac{\partial}{\partial x}\left(ph^3 Q\frac{\partial p}{\partial x}\right) + \frac{\partial}{\partial y}\left(ph^3 Q\frac{\partial p}{\partial y}\right) = 6\mu V_x \frac{\partial(ph)}{\partial x} + 6\mu V_y \frac{\partial(ph)}{\partial y} + 12\mu\frac{\partial(ph)}{\partial t}, \tag{4}$$

where h is the air bearing thickness; μ is the ambient gas viscosity; V_x and V_y are gas velocity components in the x and y directions; Q is a modification function to account for gaseous rarefaction effects.

If the effective speed of the L/UL mechanism is v, then the displacement at the L/UL point can be written as

$$z_L = vt \tag{5}$$

The suspension force applied on the slider in the Z-direction is

$$f_z = \min\left\{k_z\left[z + x_d * \cos(\theta) - z_L - z_0\right] + c_z\left[\dot{z} + x_d * \dot{\theta} - v\right], \mathrm{F}_0\right\} \tag{6}$$

and the additional forces from the offset x_d and y_d are

$$f_\theta = f_{\theta 0} + x_d * f_z \tag{7}$$

and

$$f_\beta = f_{\beta 0} + y_d * f_z \tag{8}$$

where F_0 is the normal load, and the effects of dimple offset are included in $f_{\theta 0}$ and $f_{\beta 0}$. Generally, there are two types of suspension assemblies. One has an integrated gimble

with no dimple. The other has an attached gimble with a dimple. For suspensions with no dimple, the parameters will not be changed in the L/UL process. However, for the suspensions with a dimple, the parameters would change during the process. If $f_z>0$, the dimple is in contact, and the parameters are

$$\begin{aligned} &k_z = k_{z1}, k_\theta = k_{\theta 1}, k_\beta = k_{\beta 1} \\ &c_z = c_{z1}, c_\theta = c_{\theta 1}, c_\beta = c_{\beta 1}, x_d = 0, y_d = 0 \end{aligned} \tag{9}$$

If $f_z<0$, the dimple has separated, and the parameters are

$$\begin{aligned} &k_z = k_{z2}, k_\theta = k_{\theta 2}, k_\beta = k_{\beta 2} \\ &c_z = c_{z2}, c_\theta = c_{\theta 2}, c_\beta = c_{\beta 2} \end{aligned} \tag{10}$$

During the load process, $v<0$, and one can find z_0 from $f_z=0$ when $t=0$. During the unload process, $v>0$, and one can find z_0 from $f_z= F_0$ when $t=0$.

Substituting Eqs. (6)-(8) into Eqs. (1)-(3), and simultaneously solving the equations, we can obtain the slider's response. Equations (1)-(3) are solved by using direct numerical integration. The CML Air Bearing Dynamic Simulator [6] was updated to implement the model.

III. SIMULATION

Two 50% air bearing designs (Type A and B), shown in Figure 2, were simulated for their unload performance by using the proposed model and program. Type A was mounted on the HTI 850 suspension and Type B was mounted on the HTI 1950 suspension. Both suspensions have a dimple. Finite element models of both suspensions were created to find the spring parameters when the dimple is in contact and when it is separated. The damper parameters were estimated from the measured damping ratios of the first three modes (1st bending, slider pitch and roll) of the suspensions in their free state. The simulation is very time consuming, especially at lower unload speeds when using small time steps. Therefore, we checked the effects of the time step first, and found

that 1μs is suitable for both cases. Then, the effects of the unload speed were evaluated in the range of 10~100 mm/s. We found that the speed only affects the magnitudes and doesn't affect the trend. Thus, most cases were simulated using the 50 mm/s unload speed. The offsets x_d and y_d are determined by the suspension design. They significantly affect the unload process of negative pressure sliders. From a FE model, we found that the stiffness is 276.5 N/m before the dimple separates, and 40.5 N/m after the dimple separates. The offset in the X-direction is –0.603 mm (offset toward the leading edge), and the offset in the Y-direction is very small. Therefore, we used x_d =-0.603 mm and y_d=0 in the simulation. The effects of the unload speed and x_d will be shown later. A smooth disk, was used in the simulation. The unload process was simulated at a disk radius of 44 mm with zero skew angle.

Figure 3 shows the histories for the flying attitudes and air bearing forces of the Type A slider during the unload process at 7000 RPM and the 50 mm/s unload speed. The unload process occurs in about 7 ms. From the figure, it is observed that we can divide the process into three stages. In the first stage, the air bearing force decreases from the initial load (3.5 gram) to zero. The flying height steadily increases from 50 nm to 106 nm, while the pitch changes from 220 μrad to 330 μrad. The positive pressure resultant force of the bearing decreases from 8.6 gram to 4.5 gram, and the negative pressure (suction) force decreases from 5.1 gram to 4.5 gram. The roll shows no obvious change. In the second stage, the dimple separates, and the air bearing force changes from 0 to a maximum negative value. This value, called the "lift-off force", is 0.9268 grams. The dimple separation is about 0.1916 mm. The flying height and pitch change from 105 nm to 280 nm and 330 μrad to 810 μrad, respectively. The positive and negative forces change from 4.5 to 1.5 gram and –4.5 to –2.43 gram, respectively. In the last stage, the air bearing quickly disappears in about 0.5 ms; this is called the release time. Here the flying height and pitch sharply increase to 0.1 mm and 0.1 rad during about a 0.7 ms time. The flying height of the slider's center increases from 1.09 μm to 0.200 mm. The loadbeam is moved about 35 μm. Therefore, the slider will impact the loadbeam at high speed in this

stage. Then it is possible for the slider to rebound and hit the disk. To reduce this possibility, we need to decrease the lift-off force and/or increase the release time. Figure 3 also shows that the negative pressure is not very sensitive to the slider's attitudes. The Type B slider had very similar properties at this RPM.

To decrease the lift-off force, we simulated the effect of the unload speed and disk RPM because these two parameters can be easily modified in the drives. Figure 4 shows the effects of the unload speed on the lift-off forces. The lower speeds have smaller lift-off force. In the unload speed range of 10~100 mm/s, the flying attitudes do not show obvious oscillations of the air bearing. This means the frequency range of the unload motion is much smaller than air bearing frequencies, and the suspension force applied to the slider can been considered as a static force. This also indicates that the assumptions of the model will not result in a large error.

Figure 5 shows the lift-off force of the Type A slider with respect to RPM. We can see that there is a maximum lift-off force at about 6000 RPM. The lift-off force is smaller and the release time is longer at lower RPM. Figure 6 shows the lift-off force of the Type B slider with respect to RPM. The maximum lift-off force occurs at about 2500 RPM. For this slider the lift-off force is smaller and the release time is longer at higher RPM. The effects of the offset x_d, which is determined by the suspensions, are also shown in Figs. 5 and 6. We see that the offset significantly affects the dynamics of the unload process.

IV EXPRIMENT

A. Experimental Setup

To investigate the dynamics of the slider-air bearing during the unload process, we developed an experimental system to directly measure the air bearing forces during the

unload process. The system was designed with the following considerations in mind. First, the unload mechanism must move at a constant vertical velocity. This was necessary to ensure the accurate measurement of the load beam stiffness. The importance of this will be discussed later. Second, the force transducer must have high enough resolution to measure the small air bearing forces. Third, the force transducer must have a sufficiently high bandwidth to measure any dynamic forces during unload. A bandwidth of zero to 1 kHz was desired. Finally, the system must lift the slider vertically so that a Laser Doppler Vibrometer (LDV) can measure slider attitudes during unload.

Figure 7 shows a schematic diagram of the experimental setup. The system consists of a motorized z axis stage that moves the force transducer vertically up and down. A Center for Tribology SSF-Plus tester was used to measure the AE signal and control the RPM. The AE signal was sent through a high pass analog filter with a cut off frequency of 500 kHz. A Polytec dual beam LDV was used to measure the vertical velocity of the unload actuator. After a series of measurements, it was shown that the unload actuator moved at a constant velocity of only 0.25 mm/sec. After an extensive search for commercially available load cells, it was decided that a simple aluminum cantilever affixed with strain gages would give the desired bandwidth with enough resolution to accurately measure the air bearing forces. A Calex Model 165 Bridgesensor amplified the strain gage signal with a gain of 1000. The amplified signal was then stored in a Lecroy 9304c digital oscilloscope. The force transducer was calibrated with known weights ranging from one to five grams force.

B. Experimental Method

A total of five HGA's, two type A and three Type B, were used in the experiment. A load/unload wire was formed out of 0.016-inch diameter piano wire and was glued to the load beam. The general shape of the wire can be seen in Fig. 7. A very consistent AE burst occurred at the point when the slider released from the disk. This burst was used to

trigger the acquisition. All measurements were performed at a track radius of 44 mm with a zero skew angle. For each slider, ten unload force histories were averaged at eleven different disk velocities. Recall from the simulation results that the maximum lift-off force occurred at 6000 RPM and 2500 RPM for the Type A and B, respectively. With this knowledge, the disk velocities were clustered around these values.

The averaged raw data for each RPM was further analyzed. Since the force transducer measures the superposition of both the air bearing force and the load beam force, it was necessary to subtract the load beam force form the raw data. Figure 8 shows a typical force history before the load beam force was subtracted. From this figure it can be seen that the force history was over sampled in order to give an accurate measure of the load beam stiffness. A regression analysis was performed on the final linear portion of this curve. The best-fit line was then extended through the whole data set and subtracted from the raw data to give the air bearing forces.

C. Experimental Results

Figure 9 shows the experimental force history at 7000 RPM for the Type A sliders. The trend of the unload force history is in excellent agreement with the simulated data. All oscillations in the force history are due to the disk run out as the frequency of the force oscillations identically matches those of the disk run out. The first two stages can distinctly be seen in the data. The discontinuity, or change in slope, is characterized by the separation of the dimple. A decaying high frequency oscillation can be seen at the point where the slider loses its negative pressure and releases. This oscillation has very little physical meaning other than the force transducer springing back from the sliders sudden release from the disk.

Next, the dependence of lift-off force on RPM was investigated. As stated previously, force history data was taken at eleven different disk velocities. Figures 5 and 6 show the

experimental and simulated lift-off forces for the two types of sliders. Again, the trend in the simulation agrees quite well with the experimental data. One immediately notices a critical value of disk velocity where the lift-off force reaches a maximum. Simulation and experiment both predict the same value. The Type B slider has a critical RPM of 2500 with an average experimental lift-off force of –1.01 grams. The Type A slider has an average experimental lift-off force of –1.11 grams at a velocity of 6000 RPM. It can also be seen that there is a slight shift between the simulated data and experimental data. It is believed that the different unload speeds between the simulation and experiment, offset values, disk waviness, roughness and flutter result in this shift. The two Type A sliders show good repeatability at lower RPM while there is a small amount of deviation at higher RPM. However, the Type B sliders show more deviation in the data. Type B sliders one and two show excellent repeatability while number three shows a greater deviation. This slider was measured a second time in order to confirm the first measurement. The reason for non-repeatability between samples is not known but it is not thought to be caused by measurement resolution.

Finally, we examined new slider designs in an attempt to minimize the lift-off force. Figure 10a shows a new ABS design that was able to reduce this force almost to zero, as shown in figure 10b. Further work must be done to optimize the design for other performance requirements. The design principle for reducing the lift-off force is to move the negative pressure cavity further back.

V. CONCLUSION

The dynamics of negative pressure sliders during the unload process was investigated by simulation and experiment. The CML dynamic simulator is modified to incorporate a simplified L/UL suspension model. In order to directly measure the air bearing forces during the unload process an experimental setup was built. Two sliders were simulated and measured at different RPM. The results show that:

1) There is a good correlation between the experimental results and simulation predictions. The program and experimental setup are robust for evaluating the slider air bearing design and unload process.
2) The air bearing suction forces result in dimple separation during unload. Consequently, the quick release of the air bearing results in a high speed impact between the slider and the load beam. It is possible for the slider to rebound and hit the disk.
3) The lower unload speeds have smaller lift-off force for both sliders.
4) Selecting a suitable RPM can decrease the lift-off force. However, it should be observed that different slider designs have different dependence on RPM.
5) As shown in Figure 10, the dimple separation can be entirely prevented during the unload process by properly designing the ABS, even though the sliders have large suction force and conventional suspensions are used. Details of such optimized designs will be discussed in another report.
6) Future research is required to properly model the effects of the suspension.

ACKNOWLEDGMENTS

This study is supported by the Computer Mechanics Laboratory at the University of California at Berkeley.

REFERENCES

[1] T. G. Jeong and D. B. Bogy, “An Experimental Study of the Parameters that Determine Slider-Disk Contacts During Dynamic Load-Unload,” ASME J. of Tribology, Vol. 114, No. 3, pp. 507-514, 1992.

[2] T. G. Jeong and D. B. Bogy, “Numerical Simulation of Dynamic Loading in Hard Disk Drives,” ASME J. of Tribology, Vol. 115, No. 3, pp. 307-375, 1993.

[3] P. G. Levi and F. E. Talke, " Load/Unload Investigations on a Rotary Actuator Disk Drive," IEEE Tran. of Magnetics, Vol. 28, No. 5, pp. 2877-2879, 1992.

[4] T. C. Fu and D. B. Bogy, "Slider-Disk Contacts During the Loading Process in a Ramp-Load Magnetic Disk Drive," Adv. Info. Storage Syst., Vol. 6, pp. 41-54, 1995.

[5] T. C. Fu and D. B. Bogy, "Drive Level Slider-Suspension Vibration Analysis and its Application to a Ramp-Load Magnetic Disk Drive," IEEE Tran. of Magnetics, Vol. 31, No. 6, pp. 3003-3005, 1995.

[6] M.F. Garnier, T. Tang and J. W. White, "Magnetic Head Slider Assembly," U.S. Patent No. 3,855,625.

[7] Y. Hu and D. B. Bogy, "The CML Air Bearing Dynamic Simulator," Technical Report No. 95-011, Computer Mechanics Lab., Dept. of Mechanical Engineering, Univ. of California at Berkeley, 1995.

[8] D. B. Bogy, Q. H. Zeng and L. S. Chen, "Air-Bearing Designs for Stable Performance in Proximity Magnetic Recording," Adv. Info. Storage Syst.(To be published).

[10] Q. H. Zeng and D. B. Bogy, "Stiffness and Damping Evaluation of Air Bearing Sliders and New Designs with High Damping", ASME J. of Tribology (to be published).

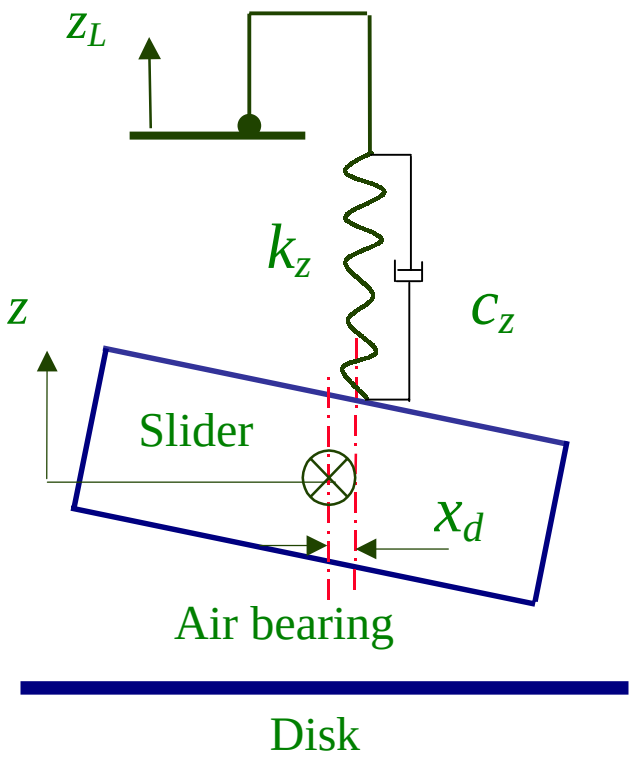

Figure 1 Slider-air bearing model for load/unload

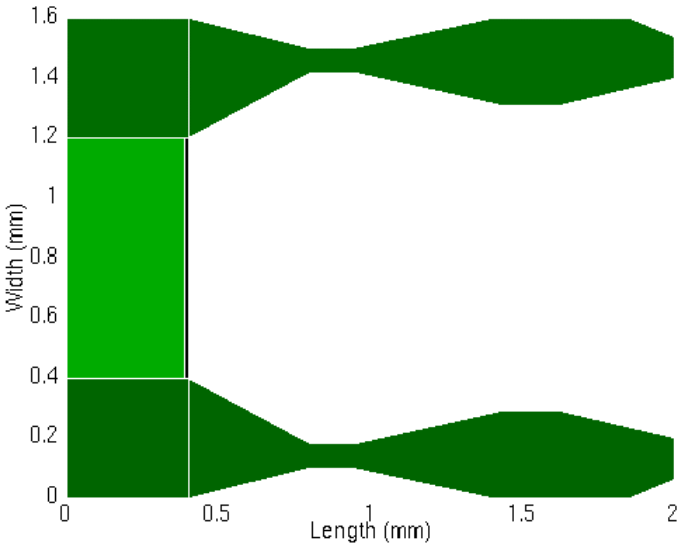

a) The Type A slider

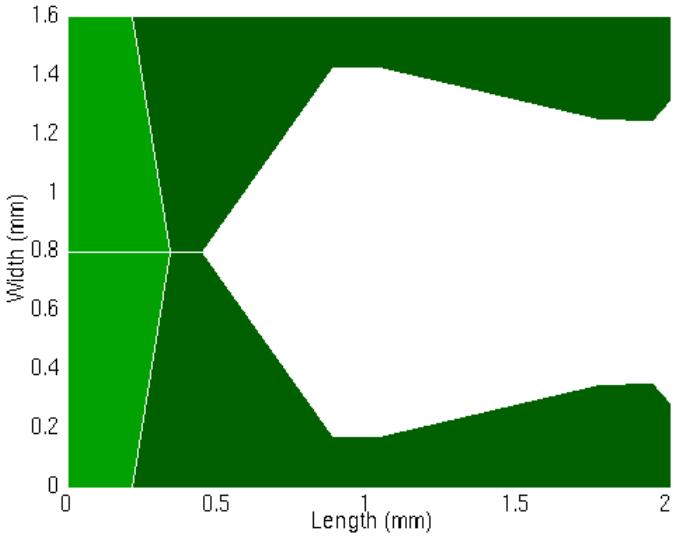

b) The Type B slider

Figure 2 Air bearing surfaces of used sliders

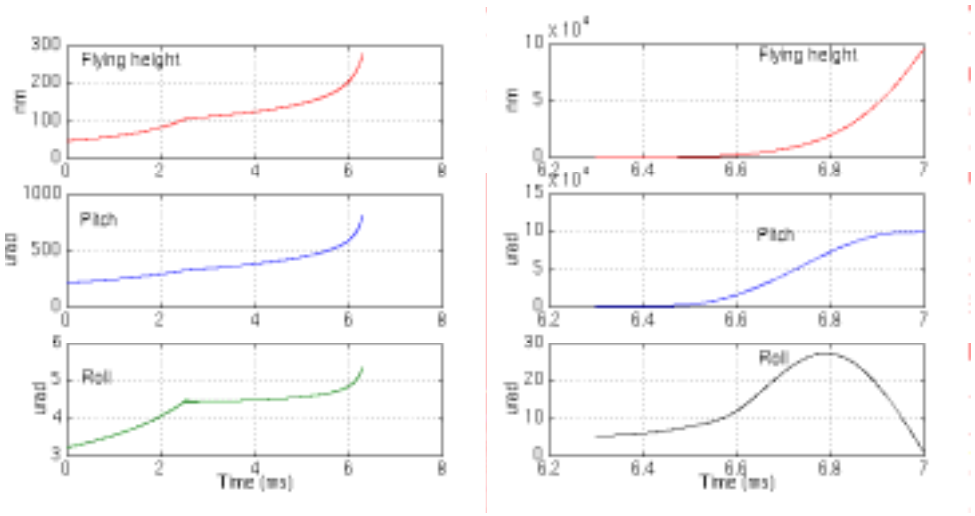

a) Flying attitudes of the slider

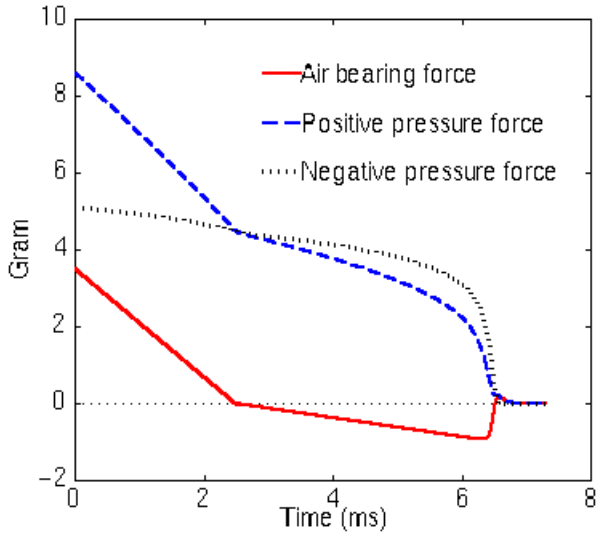

b) Force history of the air bearing

Figure 3 Calculated flying attitudes and force history of the Type A slider during the unload process (7000 RPM, 50 mm/s unload speed)

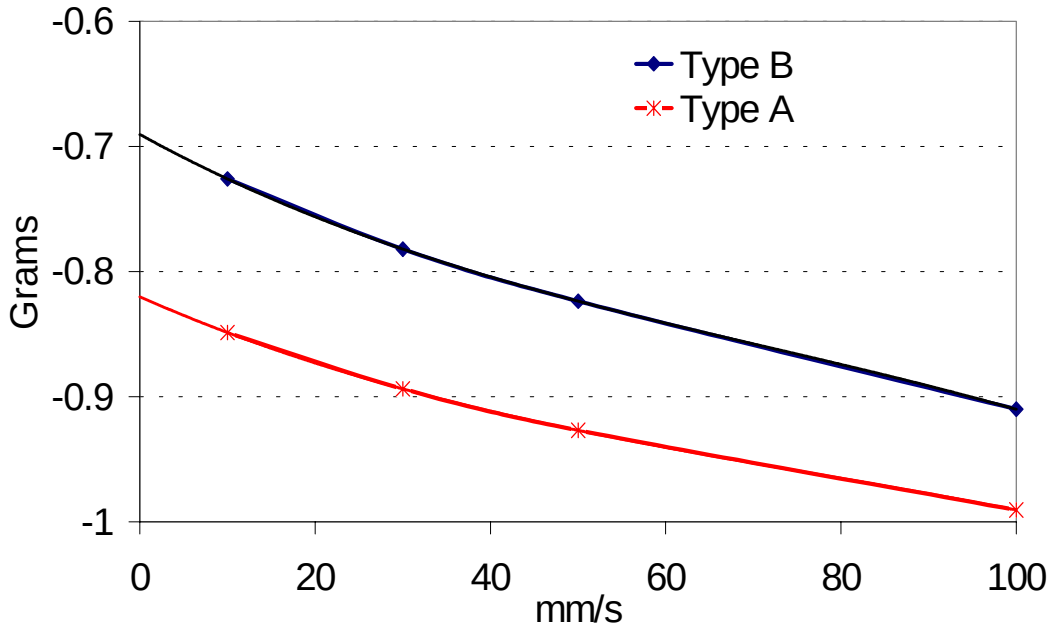

Figure 4 Calculated lift-off force with respect to the unload speed (7000 RPM, x_d=-.603 mm)

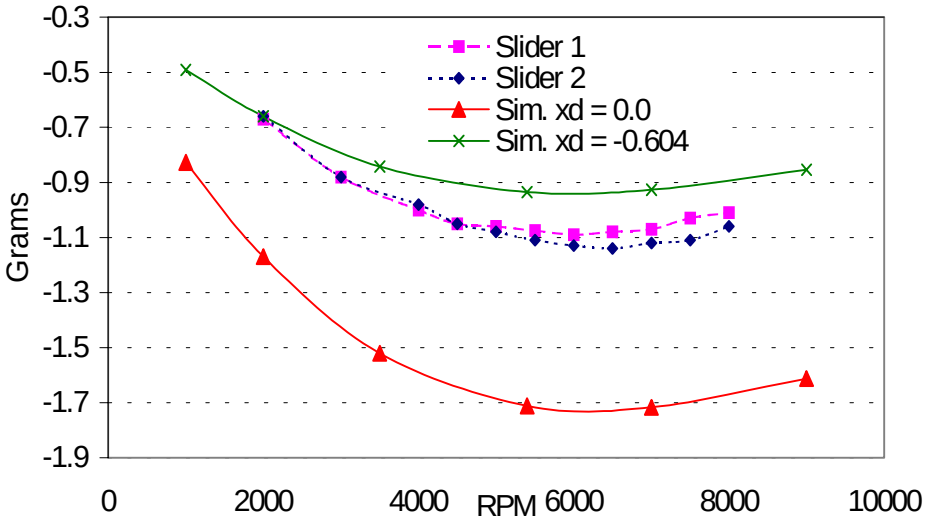

Figure 5 Measured and calculated lift-off force of the Type A slider

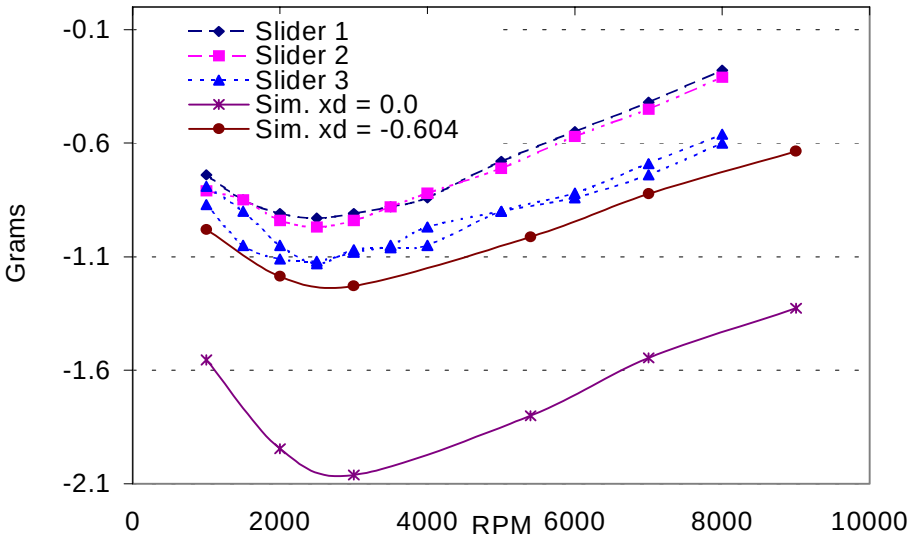

Figure 6 Measured and calculated lift-off force of the Type B slider

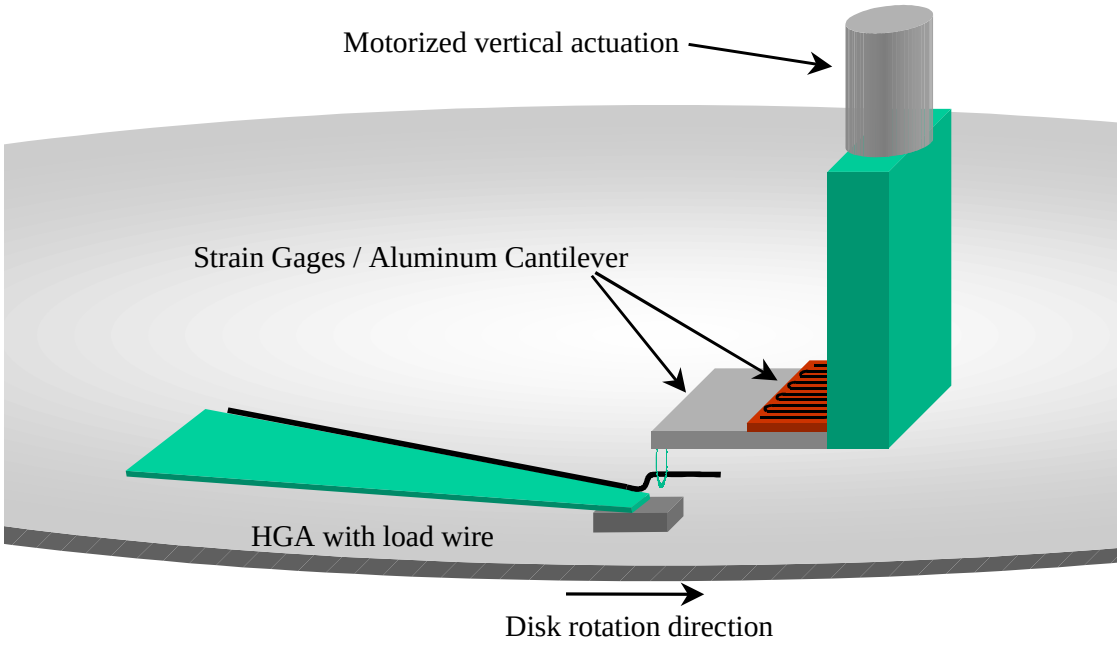

Figure 7 Experimental setup

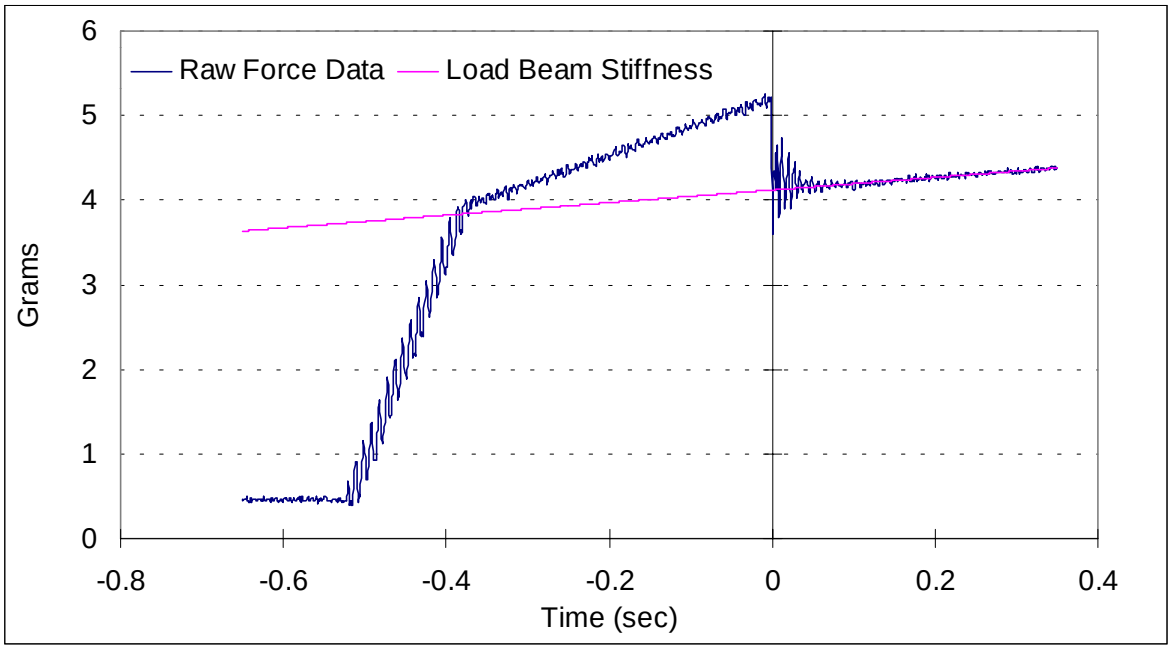

Figure 8 Unload force history before load beam force is subtracted

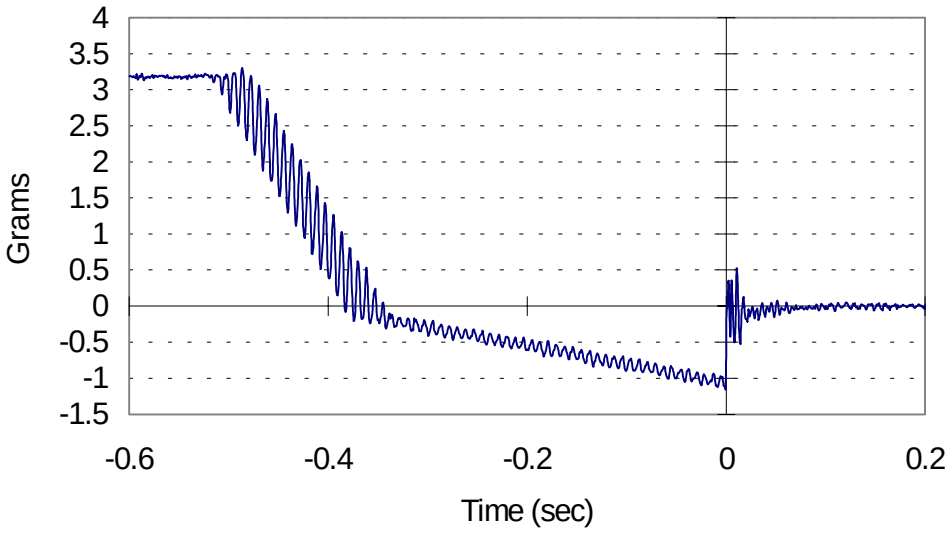

Figure 9 Measured unload force history for the Type A Slider at 7000 RPM

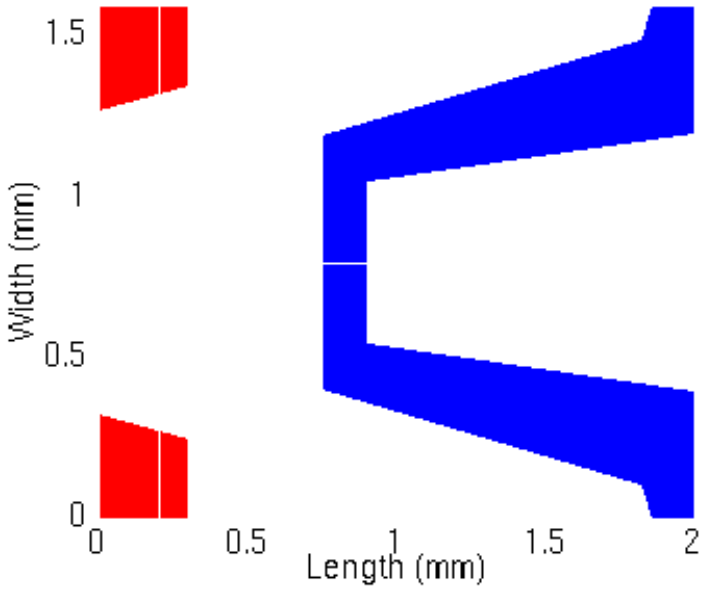

a) Air beaing surface

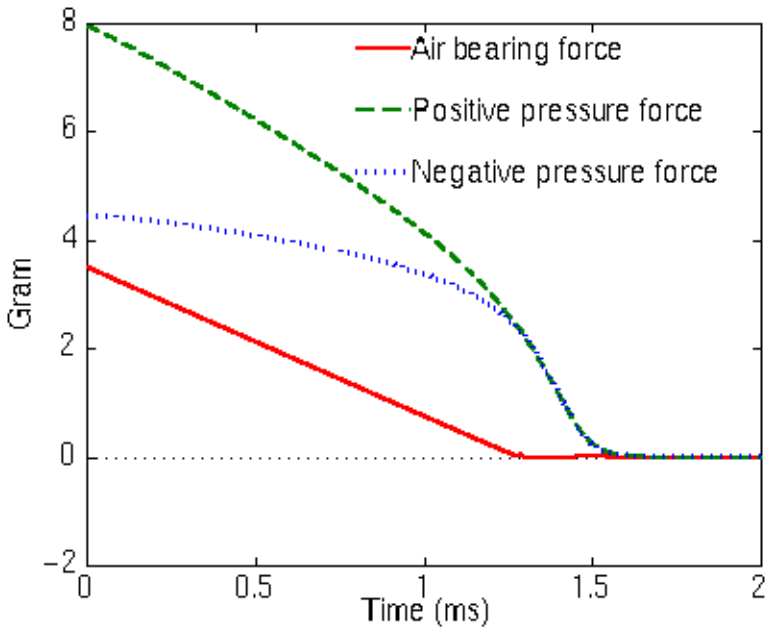

b) Air Bearing force (7000 RPM)

Figure 10 Air bearing surface design for L/UL